

# Non-linear Models for the Deformation of Cellular Structures

Jagir R. Hussan<sup>\*1</sup>, Gaven J. Martin<sup>2</sup>

<sup>1</sup>Auckland Bioengineering Institute, University of Auckland, New Zealand

<sup>2</sup>New Zealand Institute of Advanced Studies, Massey University, New Zealand

<sup>\*</sup>r.jagir@auckland.ac.nz; <sup>2</sup>G.J.Martin@massey.ac.nz

## Abstract

Motivated by the ubiquity Dirichlet like energy functionals in cellular physics, we study deformations of such systems, specifically the constraints governing the interface changes. We prove, in general, that the problems of minimisation of local mean angular distortion and Dirichlet energy are identical (up to a measure). In a more restricted regime of hexagonal tessellations, non-existence of minimisers for non-linear deformations has been demonstrated.

## Keywords

Nonlinear Models; Deformations; Cellular Structures; Quasiconformal

## Introduction

The Dirichlet energy functional, below at (1) is common in many areas of physics.

$$\mathcal{E}(f) = \frac{1}{2} \int_{\Omega} |\nabla f|^2 dx. \quad (1)$$

Extremal solutions to (1) have been shown to govern stable packing's in 2D structures and cylinders (Bezdek and Kuperberg, 1990; Cafferelli and Lin, 2007; Cybulski and Hołyst, 2005) and implicitly satisfy structural stability conditions (Mullins, 1963; Von Neumann, 1952).

Further, in the so-called equal-constant setting in liquid crystal theory the Frank-Oseen energy (Oseen, 1933; de Gennes and Prost, 1993; Virga, 1994) reduces to (1). Often, the stability and configuration of such structures under deformations/change of boundary conditions are desired.

This report is concerned with theoretical mathematical models to analyse the deformation of 2D cellular structures such as one might observe as a cross section of tissue, or in various models of foams and elsewhere, See (Weaire and Hutzler, 1999; Weaire and Rivier, 2009). In the latter case, particularly soap foams, the theory of conformal mappings has been used to

various effect (Drenckhan et al., 2004; Mancini and Oguey, 2005). In cases where free boundary conditions do not always exist, the extension of such approaches to fixed boundary conditions, where conformal maps do not always exist, is desired.

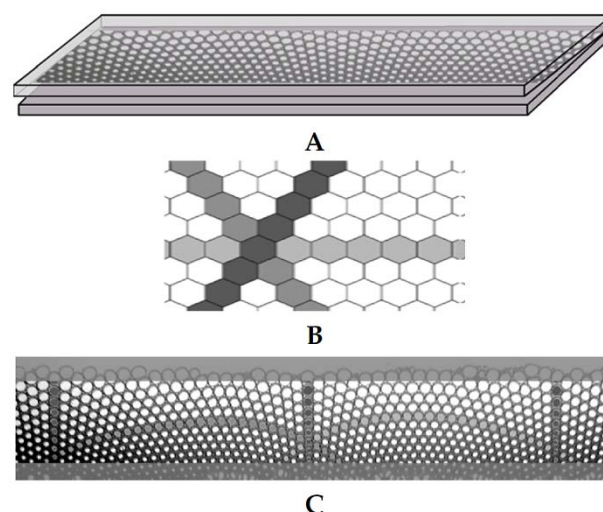


FIG 1 EXPERIMENTAL RESULTS FOR BUBBLES TRAPPED BETWEEN TWO GLASSPLANS. A. PLATE CONFIGURATION, THE BOTTOM PLATE IS HORIZONTAL AND THE TOP IS SLIGHTLY TILTED. B. COMPUTER GENERATED HONEYCOMBSTRUCTURE WITH SHADING PATTERN TO AID VISUALISATION OF TRANSFORM EFFECTS. C. EXPERIMENTALLY OBSERVED PATTERN FOR THE PLATE CONFIGURATION. THE CONFORMAL TRANSFORM FROM  $B \rightarrow C$  IS  $w = (i\alpha)^{-1} \log(iaz)$ , HERE  $2\pi/\alpha$  IS THE TRANSLATIONAL PERIOD.

Reproduced from Figure 1 and 3 from (Drenckhan et al., 2004)

## Motivation

The case of deforming soap films is discussed as it will partially motivate the approach we take. A deformation of a 2D-cellular structure of soap films is achieved in the following manner: consider the cellular structure of soap bubbles- finite in extent - trapped between two close parallel panes of glass (Fig. 1B). The steady state with bubbles of uniform size is closely approximated by a regular 2D hexagonal

tessellation. Vary the angle between the panes. The new configuration is expected to be achieved by a conformal deformation for two reasons.

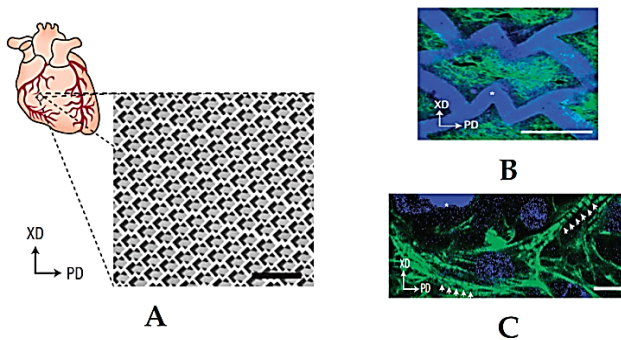


FIG 2 A. SCHEMATIC OF ACCORDION-LIKE HONEYCOMB STRUCTURE. B. F-ACTIN LABELLED NEONATAL RAT HEART CELLS (CULTURED FOR 1-WEEK). C. MAGNIFIED VIEW OF THE CELL CULTURE. THE LABELLING IDENTIFIES STRESS FIBRES; THE WHITE ARROWS MARK THE CROSS-STRIATIONS. PD AND XD ARE THE PREFERRED AND ORTHOGONAL CROSS-PREFERRED MATERIAL DIRECTIONS. THE DIRECTIONS ALIGN WITH THE CIRCUMFERENTIAL AND LONGITUDINAL FIBRE DIRECTIONS respectively. Scale bars A. 200  $\mu\text{m}$ , B. 100  $\mu\text{m}$ , and C. 10  $\mu\text{m}$ . Reproduced from Figure 2 and 3 of Engelmayer Jr. et al., 2008.

Firstly, the equations to minimize the interfacial (film) energy give, locally, a trivalent equal angle of  $2\pi/3$  hexagonal tiling. Secondly, there are no boundary constraints. Since the initial configuration also exhibits  $2\pi/3$  symmetry, scale invariance and pressure/volume considerations suggest that the free boundary “free energy minimisation” problem may be solved by an angle preserving deformation- that is a conformal mapping. Thus it might be expected that the Euler-Lagrange equations to be the *linear* Cauchy-Riemann equations. Conformal mappings are also absolute minimisers of Dirichlet energy in the free boundary case- an elementary consequence of Hadamard's inequality. Therefore the appearance of the Dirichlet energy functional is expected. Of course the connection between conformal mappings and harmonic functions is well known.

Next, in a more constricted regime, one might use microfabrication techniques to create accordion-like honeycomb microstructure to yield porous, elastomeric three-dimensional scaffolds with controllable stiffness and anisotropy (Fig. 2) as in Engelmayer Jr. et al., 2008. In that paper the authors have demonstrated that the neonatal rat cardiac cell based tissue, cultured using these honeycomb scaffolds, closely matched the mechanical properties of rat ventricular myocardium and that heart cell contractility was inducible by electric field stimulation

with directionally dependent electrical excitation thresholds showing that honeycombs can overcome some of the main structural limitations of previous approaches. Here there is a relatively stiff interface - scaffolding structure - being deformed *at the boundary* and quite different effects are modelled.

### Objective

Our aim here is to present a first attempt at a “holistic” mathematical formalism which might encompass theoretical analysis structures which appear at both ends of the spectrum. The film models could be extended in various ways. In particular, we should

- allow the model to include boundary conditions on the interface -such as stretching, shearing, or other deformations.
- allow different functionals related to the elastic tension of the interface
- allow for the internal structure of each cell - after deformation- to rearrange itself to minimise some “free energy” functional (which may vary from cell to cell). These functionals may range from (1) to fully nonlinear (possibly degenerate) variational type energies and could reflect possible internal cellular structure.

Of course, the energy functional characterising tissues is rather more complex and we should only expect a fairly coarse analogy- however, near steady state most symmetries and integral invariants are conserved and we will be able to assert existence and regularity of minimisers of our models in reasonable physical situations. We will also see interesting features regarding the singular structure of the solution across the interface.

A discussion on the model's relationship to known physics of multicellular structures, the predictability of observables such as interface structure, minimal loss of symmetry, regularity and so forth under deformation will be considered.

There is one other aspect we will investigate. Many naturally occurring functionals have Morrey's quasiconvexity property (Morrey Jr., 1966), not discussed in detail here, but it is basically an assumption that makes the “direct method” in the calculus of variations work- minimising sequences have a limit which is a minimiser. Roughly it asserts the assumption that if a linear mapping is a candidate for the minimisation problem (for instance linear boundary values), then this linear mapping is the minimiser. In 2D, Dirichlet energy obviously has this

property as linear mappings are harmonic. Quasiconvexity is a natural property of many physically motivated functionals, but linear mappings are not conformal so some differences are expected to be observed.

### The Structure of the Model

2D-regions in the complex plane tessellated by regular hexagons and subjected to a boundary deformation are considered. It is assumed that the boundary deformation propagates to the interior instantaneously to minimise the average angular distortion at interfacial vertices. Then the interface relaxes to minimise some local energy functional, for instance pressure differences across the interface. This then moves the interface (and possibly some internal cellular organisation) into an extremal configuration.

Surprisingly we will be able to solve this problem in the sense we will identify the initial vertex configuration (the average angle minimising deformation with given boundary values) and discover a curious connection with harmonic mappings – though the minimiser will *not*, in general, be harmonic.

Motivated by the fact that conformal mappings preserve angles we consider the case where the boundary deformation propagates to the interior to minimise the maximum angular distortion. It will follow from our analysis below, that this problem has a solution (that is a deformation of minimal distortion exists) but it may not be unique or particularly regular.

There are a few things of note in our model. First, we should expect the maximum distortion of the honeycomb lattice should occur at the boundary. Our model will verify this. Second, we should expect that our model does not have a completely regular minimiser - we should expect some singular structures to define the interface. We will also see this in our model.

### The Duality Between Local Angular Distortion and Dirichlet Energy

As we indicated in the introduction, conformal mappings may arise as energy minimising deformations for two reasons. First, they do not distort (at an infinitesimal level) angles and second, that they are absolute minimisers of Dirichlet energy.

It is the purpose of this subsection to mathematically

derive this very interesting relationship.

In Astala et al, 2010 a connection between distortion of relative lengths (linear dilatation) and Dirichlet energy was observed. Here we explicitly relate these quantities to angular distortion.

Consider a deformation  $f$  of a planar region  $\Omega \subset \mathbb{C}$ . Analytical investigations of deformations require some degree of smoothness. Henceforth, it is assumed that  $f \in W_{loc}^{1,2}(\Omega, \mathbb{C})$ , that is locally (at each point there is a small region where) the first derivatives exist as locally square integrable functions. Be aware that such a regularity assumption does not even guarantee that the deformation is continuous. The reader may acquaint themselves fully on the modern aspects of the theory of planar deformations in Astala et al, 2010. The reader well versed in the analytic theory will see that for the most part (and entirely for certain functionals) it is possible to work with the much larger, and far less regular, class of  $W_{loc}^{1,1}$ -Sobolev mappings.

### Angular Distortion Functionals

The local angular distortion is a function of the differential map – the best local linear approximation to a deformation at a given point.

To motivate our considerations we start with an analysis of the angular deformation by linear maps. A linear mapping has the form  $f(z) = az + b\bar{z}$ ,  $a, b \in \mathbb{C}$ . The deformation is assumed orientation preserving and injective so  $|a| > |b|$ . The injectivity assumption is physically motivated by the principle of “interpenetrability of matter”.

Of course conformal rotation and scaling does not change local angular deformation so we may as well consider the linear map with  $\mu = a/b$ .

$$z \mapsto z + \mu\bar{z} \quad (2)$$

for our analysis.

The maximum and minimum angular distortion for the linear map are

$$\max_{\theta \in [0, 2\pi]} \left| \frac{d}{d\theta} (e^{i\theta} + \mu e^{-i\theta}) \right|, \quad \min_{\theta \in [0, 2\pi]} \left| \frac{d}{d\theta} (e^{i\theta} + \mu e^{-i\theta}) \right|. \quad (3)$$

Identifying that

$$\begin{aligned} \left| \frac{d}{d\theta} (e^{i\theta} + \mu e^{-i\theta}) \right|^2 &= |ie^{i\theta} - i\mu e^{-i\theta}|^2 = |1 - \mu e^{-2i\theta}|^2 \\ &= 1 + |\mu|^2 - 2\Re(\mu e^{-2i\theta}). \end{aligned} \quad (4)$$

Accordingly,

$$\max_{\theta \in [0, 2\pi]} \left| \frac{d}{d\theta} (e^{i\theta} + \mu e^{-i\theta}) \right| = 1 + |\mu|, \quad (5)$$

$$\min_{\theta \in [0, 2\pi]} \left| \frac{d}{d\theta} (e^{i\theta} + \mu e^{-i\theta}) \right| = 1 - |\mu|. \quad (6)$$

Defining the angular distortion as the ratio of these quantities (which would be natural in some sense) has a problem for us from the point of view of variational calculus. Certainly conformal mappings are absolute minimisers as  $\mu \equiv 0$ . However  $\mu = 0$  is not a smooth minimum (in the sense that  $\frac{d}{ds} \left( \frac{1+s}{1-s} \right) \Big|_{s=0} = 0, \mu \equiv 0$ , and to study variational problems it is almost essential that the functional has smooth minima so as to be able to derive Euler-Lagrange equations and so forth.

For this reason, consider the ratio of  $1 + |\mu|^2$  and  $1 - |\mu|^2$  instead. Then, as  $\frac{d}{ds} \left( \frac{1+s^2}{1-s^2} \right) \Big|_{s=0} = 0, \mu \equiv 0$  will be a smooth minimum.

Since the function  $t \mapsto t + 1/t$  is convex and increasing for  $t \geq 1$ , the maps which pointwise minimise the ratio  $(1 + |\mu|)/(1 - |\mu|)$  and those which minimise  $(1 + |\mu|^2)/(1 - |\mu|^2)$  are identical.

However, minimising integral averages reveals surprising differences.

### Generalised Distortion Functionals

The above discussion can be cast in a more general framework as follows.

For a deformation  $f \in W_{loc}^{1,2}(\Omega, \mathbb{C})$ , define the Beltrami coefficient

$$\mu_f(z) = \frac{f_{\bar{z}}(z)}{f_z(z)} \quad (7)$$

The theory of quasiconformal mappings and Beltrami equations assumes the uniform bounds  $\|\mu(z)\|_{L^\infty(\Omega)} = k < 1$  leading to a “uniformly elliptic” theory. However recent advances (Iwaniec and Martin, 2008) allow for the consideration of degenerate elliptic theory which seems more suitable in situations where *a priori* bounds will not be easy to achieve.

Note that  $\mu \equiv 0$  implies  $f_{\bar{z}} = 0$  (the Cauchy-Riemann equations) and the regularity assumptions imply  $f$  is conformal-angle preserving. On defining the distortion measure as the average of the ratios of the largest to smallest and smallest to largest angular distortion:

$$\mathbb{A}(z, \cdot) = \frac{1}{2} \left( \frac{\max_{\theta \in [0, 2\pi]} \left| \frac{d}{d\theta} \cdot \right|}{\min_{\theta \in [0, 2\pi]} \left| \frac{d}{d\theta} \cdot \right|} + \frac{\min_{\theta \in [0, 2\pi]} \left| \frac{d}{d\theta} \cdot \right|}{\max_{\theta \in [0, 2\pi]} \left| \frac{d}{d\theta} \cdot \right|} \right). \quad (8)$$

The calculations applied to the linear differential of  $f$  show that

$$\mathbb{A}(z, f) = \frac{1 + |\mu_f(z)|^2}{1 - |\mu_f(z)|^2}. \quad (9)$$

In fact it turns out that  $\mathbb{A}(z, f)$  not only controls the angular distortion of a mapping, but also its linear distortion.

**Example 1.** For  $z_0 \in \Omega$  and  $0 < r < \text{dist}(z_0, \partial\Omega)$ , set

$$L(r) = \max_{|z|=r} |f(z) - f(z_0)|, \quad \ell(r) = \min_{|z|=r} |f(z) - f(z_0)|$$

to be the largest and smallest stretching at scale  $r$  for the mapping  $f$ . Define

$$K(z_0, f) = \limsup_{r \rightarrow 0} \frac{L(r)}{\ell(r)} \quad (10)$$

the linear dilatation of  $f$  and, for reasons of convexity again, define a pointwise ratio

$$\mathbb{K}(z, f) = \frac{1}{2} \left( K(z, f) + \frac{1}{K(z, f)} \right). \quad (11)$$

It is easy to verify that for a linear mapping  $z \mapsto az + b\bar{z}$  the number  $K$  is simply the ratio of the larger to the smaller axes of the ellipse  $f(\mathbb{S}(z_0, r))$  – the deviation from roundness or eccentricity of the image.

The following theorem is easy following the discussion for linear maps – but nonetheless quite remarkable. It shows that the quantities measuring angular distortion and deviation from the “preservation of roundness” are the same.

**Theorem 1.** Let  $f: \Omega \rightarrow \mathbb{C}$  be a homeomorphism of Sobolev class  $W_{loc}^{1,1}(\Omega, \mathbb{C})$ .

Then

$$\mathbb{A}(z, f) = \mathbb{K}(z, f) \quad \text{almost everywhere in } \Omega \quad (12)$$

*Proof.* Using (7), (10) in (11) and simplifying gives

$$\mathbb{K}(z, f) = \frac{|f_z|^2 + |f_{\bar{z}}|^2}{|f_z|^2 - |f_{\bar{z}}|^2} = \frac{\|Df\|^2}{J_f} = \mathbb{A}(z, f) \quad (13)$$

where  $\|\cdot\|$  is the Hilbert-Schmidt norm of the differential and  $J_f$  is the Jacobian determinant. The distortion function  $\mathbb{K}$  is discussed extensively in Astala et al, 2009.

The reader should not be too concerned with the “almost everywhere” part of the theorem. It is a consequence of working with nondifferentiable Sobolev functions – so the quantities involved are only defined on a set of full Lebesgue measure. If  $f$  is a



diffeomorphism, then the equality holds everywhere.

Eq. (13) provides the first possible connection between the Dirichlet energy and angular or spherical distortion. This is formalised in the following theorem. The proof is a triviality apart from the quite deep technical complexity in using the change of variables formula for mappings in the stated Sobolev class. This change of variables in greater generality than we need – for mappings of finite distortion where  $\mathbb{K}(z, f) < \infty$  almost everywhere – has been established by Hencl and Koskela, 2006.

**Theorem 2.** Let  $f: \Omega \rightarrow \tilde{\Omega}$  be a homeomorphism of Sobolev class  $W_{loc}^{1,1}(\Omega, \tilde{\Omega})$  and suppose that  $\mathbb{A}(z, f)$  is a locally integrable function. Set  $g = f^{-1}: \tilde{\Omega} \rightarrow \Omega$ . Then  $g \in W_{loc}^{1,2}(\tilde{\Omega}, \Omega)$  and

$$\iint_{\Omega} \mathbb{A}(z, f) dz = \iint_{\tilde{\Omega}} \|Dg(w)\|^2 dw \quad (14)$$

*Proof.* Change variables by  $g$  in the integral at (14).

$$\begin{aligned} \int_{\Omega} \mathbb{A}(z, f) dz &= \int_{\Omega} \frac{\|Df(z)\|^2}{J(z, f)} dz \\ &= \int_{\tilde{\Omega}} \frac{\|Df(g(w))\|^2}{J(g(w), f)} J(w, g) dw \\ &= \int_{\tilde{\Omega}} \frac{\|Df(g(w))\|^2}{J(g(w), f)J(w, g)} J(w, g)^2 dw \\ &= \int_{\tilde{\Omega}} \|Df(g(w))\|^2 J(w, g)^2 dw \\ &= \int_{\tilde{\Omega}} \|Df(g(w))J(w, g)\|^2 dw \\ &= \int_{\tilde{\Omega}} \|(Dg(w))^{-1}J(w, g)\|^2 dw \\ &= \int_{\tilde{\Omega}} \|Dg(w)\|^2 dw. \end{aligned}$$

Here, the obvious facts are that  $f(g(w)) = w$ , so  $Df(g)Dg = \mathbb{I}$  and the Jacobian determinants satisfy  $J(g(w), f)J(w, g) = 1$  and the less obvious fact is that

$$\begin{aligned} \|Df(g(w))J(w, g)\|^2 &= \|(Dg(w))^{-1}J(w, g)\|^2 \\ &= \|Dg(w)\|^2 \end{aligned} \quad (15)$$

Note that here it is not the matrices which are the same, merely their norm. This fact can be established via an eigenvalue argument.

## Observations and More General Models

Listed below are some observations, theorems, assumptions and simplifications that enable the development of a general model.

### Existence and Regularity

Theorem 2 (and in particular (14)) shows that

minimisers of mean angular distortion have inverses which are minimisers of the Dirichlet energy – harmonic mappings. In particular we have (following §21.1.5 Astala et al, 2010)

**Theorem 3.** Let  $\Omega \subset \mathbb{R}^2$  be a convex domain and  $f_0 \in \mathcal{F}(\Omega, \tilde{\Omega})$ .

Then the minimisation problem has a unique solution. This extremal map is a  $\mathbb{C}^\infty$ -diffeomorphism whose inverse is harmonic in  $\tilde{\Omega}$ .

$$\min_{f \in \mathcal{F}} \iint_{\Omega} \mathbb{A}(z, f), \quad f = f_0 \text{ on } \partial\Omega, \quad (16)$$

We sketch a proof of this as follows. First, we may assume using the Riemann mapping theorem, that the target domain is the disk. This is because if  $\varphi: f_0(\Omega) \rightarrow \mathbb{D}$  (notation explained momentarily) is conformal, then  $\mathbb{A}(z, f) = \mathbb{A}(z, \varphi \circ f)$  since  $\varphi$  does not distort angles. Therefore we can solve the minimisation problem for the boundary values  $\varphi \circ f_0$  with a smooth diffeomorphism  $f$ , then the solution we want is  $\varphi^{-1} \circ f$  with boundary values  $f_0$ . So we assume  $f_0(\Omega) = \mathbb{D}$  and set  $g_0 = (f_0)^{-1}$ . The harmonic extension of  $g_0|_{\partial\mathbb{D}} \rightarrow \partial\Omega$  (call it  $g$ ) is a smooth diffeomorphism (given by integration against the Poisson kernel), see Duren, 2004. Here convexity of the image  $\Omega$  of  $g_0$  is needed and the smoothness and non-vanishing of the Jacobian determinant is a classical result known as Choquet's Theorem (Duren, 2004). Now  $g$  minimises the Dirichlet energy and so (14) tells us that  $f = g^{-1}$  solves our minimisation problem for mean angular distortion. The uniqueness of Dirichlet minimisers for the boundary value problem tells us that  $f$  is unique.

### 1) Maximum Distortion at the Boundary

In Martin et al, 2009, it is shown that if  $f: \mathcal{U} \rightarrow \mathbb{R}^2$  is a homeomorphism defined in some region and if the inverse of  $f$  is harmonic, then  $\mu = \mu_f = f_{\bar{z}}/f_z$  satisfies the nonlinear Beltrami equation

$$\bar{\mu}_{\bar{z}} = \mu \bar{\mu}_z \quad (17)$$

Since  $f$  will be a diffeomorphism,  $|\mu(z)| < 1$  and (17) shows  $\mu$  to be locally quasiregular (for the theory of such mappings, see Astala et al, 2010). In particular  $\mu: \mathcal{U} \rightarrow \mathbb{R}^2$  is an open mapping and therefore satisfies the maximum principle. That is  $|\mu(z)|$  is largest on the boundary of  $\mathcal{U}$ . Since  $\mathbb{A} = \frac{1+|\mu|^2}{1-|\mu|^2}$  the maximum angular distortion also occurs on the boundary.

### 2) Internal Structures of the Domain

The above calculations in Section Generalised-

distortion-functionals and in particular (14) was made for Lebesgue measure. It carries over with obvious changes in the formula for other measures  $\lambda(z)dz$ . That is we have

$$\iint_{\Omega} \mathbb{A}(z, f) \lambda(z) dz = \iint_{\Omega} \|Dg(w)\|^2 \lambda(g(w)) dw \quad (18)$$

for bounded  $\lambda$ . Minimisers of the right-hand side of (18) are harmonic with respect to the metric  $\lambda(z)dz$ . There are many aspects of this more general theory (existence and uniqueness and so forth) that are relevant to our investigation in this more general setting, see Schoen and Yau, 1997. In particular, this mechanism can be applied to relate mappings which are harmonic with respect to other metric structures and mappings which minimise a weighted mean angular distortion. This weight can be used to mimic internal structures of the domain.

### 3) Other Local Functionals

In what follows, minimisation of Dirichlet energy and harmonic mappings, or elementary considerations about pressure/volume and the relationship with interfacial curvature will be used as the simplest examples of the general models. However, there are other natural - and physically motivated functionals - which one might consider and will lead to a good theory. The prototypical such linear functionals are those of divergence form:

$$\mathcal{E}[f] = \iint_{\Omega} \langle A(z) \nabla f, \nabla f \rangle dz \quad (19)$$

with second order Euler-Lagrange equations  $A(z)\nabla f = 0$ . Here  $A(z)$  is a measurable positive definite symmetric matrix - Dirichlet energy and Laplace's equation is obtained for  $A = \mathbb{I}$ , the identity matrix.

$A$  can be viewed as organising the internal structure of a region, as happens in impedance tomography and the associated Calderon problem (§18 Astala et al, 2010). Here  $A$  is viewed as a density function and various substructures are identified by their relative densities (as a measurable function,  $A$  need not vary continuously - discontinuous changes in density identify interfaces internal to the cellular structure).

More difficult would be nonlinear examples minimising  $\langle A(z, f) \nabla f, \nabla f \rangle$  or related functionals. Here, there are significant technical difficulties, but some things can be done under stronger smoothness assumptions on  $A$ . The linear theory is aided by such things as Liouville's Theorem that

bounded entire, that is defined everywhere on  $\mathbb{C}$ , solutions are constant. And removable singularity type theorems, so solutions can be extended as solutions over isolated points under mild assumptions (boundedness for instance). In the linear theory, these things follow from the quasiconformal theory by harmonic factorisation theorem established in (§16.1.4 Astala et al, 2010) which also gives optimal regularity.

### 4) Admissible Boundary Deformations

Our model now describes how the initial deformation may propagate into the interior. This deformation  $f$  with boundary values  $f_0$  gives us a "nonlinear" hexagonal tessellation of the interior.

The procedure will now be used to relax this nonlinear tessellation to minimise some free energy functional (discussed next). There are two issues to consider here. First concerns the local regularity of the boundary values. It is a simple consequence of a result of Martio and Pavlovic, see (Martio and Pavlovic, 2002) and our analysis in section Generalised-distortion-functionals relating linear and angular distortion, that the angular distortion of this extension is bounded if and only if the boundary values of  $f_0$  are bilipschitz.

That is there must be a constant  $L$  so that

$$\frac{1}{L} |x - y| \leq |f_0(x) - f_0(y)| \leq L |x - y| \quad \text{for all } x, y \in \partial\Omega \quad (20)$$

Roughly this says that the derivative of  $f$  is bounded and has bounded reciprocal. Strictly one needs some smoothness assumptions on  $\partial\Omega$  for this, say smooth and convex. Since there seems little physical motivation to consider cases where there might be infinite angular distortion we accept this condition. Another problem is slightly more subtle. Namely a large scale deformation which is locally regular may lead to a vertex configuration which cannot be relaxed without the interface exiting the domain. For instance when  $f_0(\Omega)$  is "highly" non-convex we expect our relaxation procedure to fail as illustrated in Figure 3.

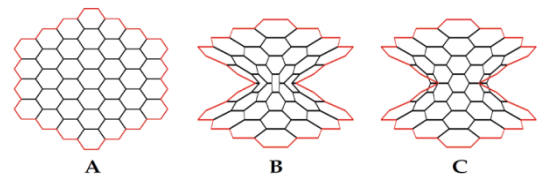


FIG 3 FAILURE OF RELAXATION PROCEDURE FOR A NON-CONVEX DEFORMATION. A. DOMAIN  $\Omega$  WITH  $\partial\Omega$  COLOURED RED. B. A NON-CONVEX DEFORMATION OF  $\Omega$ . C. RELAXATION CAUSES EDGES TO SPILL BEYOND THE FIXED BOUNDARY.

There are basically two ways forward. That is to assume the deformation  $f_0$  has bilipschitz constant (the number  $L$  in (20)) close to one. Alternatively we might assume that the deformation  $f_0$  itself has a regular image (say again convex).

### The Interfacial Energy Functional

The extension of our boundary values to a deformation of the domain  $\Omega$  gives us a finite mesh (collection of vertices and curvilinear edges joining them). A connection free energy or interfacial energy can be defined as follows. Each vertex  $v$  is associated with a finite number of arcs  $e_i, i = 1, 2, \dots, n$ , emanating from it (a hexagon model will have  $n = 3$ ). Let  $\ell(e_i^v)$  denote the length of this arc.

Define

$$\mathcal{E}_L = \sum_{\text{vertices } v} \sum_{i=1}^n \ell(e_i^v). \quad (21)$$

This energy penalises arc length, and it is clear that the sum immediately decreases when each arc is replaced with the line segment joining its endpoints.

This is a physically relevant model since the interfacial (mean) curvature is a measure of the pressure differential across the interface. In an energy minimising configuration we expect this pressure differential to be 0 so the curvature of the interface should be 0, that is the interface should be locally made of line segments (in 2D).

Here one could explore to useful purpose, other increasing functions of the edge length. For instance, define  $\Phi(t)$  to be increasing on  $[0, \infty]$ ,  $\Phi(0) = 0$ , and define the  $\Phi$ -connection free energy by

$$\mathcal{E}_\Phi = \sum_{\text{vertices}} \sum_{i=1}^n \Phi(\ell(e_i)) \quad (22)$$

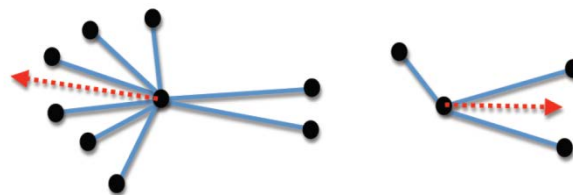
Again, as  $\Phi$  is increasing, arcs can be replaced by line segments to decrease free energy.

For a mesh which consists of line segments with trivalent vertices, all the internal angles are  $2\pi/3$  at a minimum of  $\mathcal{E}_L$ .

If not, consider a vertex where this is not the case. Choose the smallest of the three angles and move the vertex into that region in the direction bisecting that angle - keeping all other vertices fixed. A simple first order analysis shows that if this angle is not  $2\pi/3$ , then the sum of edge length decreases. A key feature here is the linearity of the connection free energy.

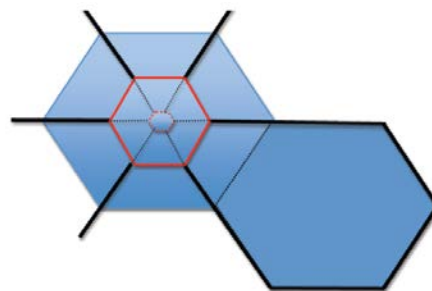
The symmetry of this critical point is not found for other functional as at (22), for instance  $\Phi(t) = t^n, n > 1$ , unless there is a very special configuration of edge lengths (again easily verified by a first order analysis). Further, it is easy to prove that for multivalency, the equal angle configuration is a local minimum.

But for the configuration obtained after a deformation, it is not easily seen what the best direction to move a vertex is, and it is certainly not always into the region with smallest angle (as illustrated below).



DIFFERENCES FOR MULTIPLE AND 3 VERTEX PROBLEM.

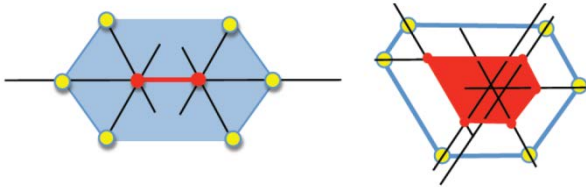
On the left-hand side, the optimal direction is not into the small estangle as the contributions from the many other vertices decrease the overall sum. On the right-hand side, for three vertices moving into the minimal angle lowers energy.



AN EVAPORATING HEXAGON.

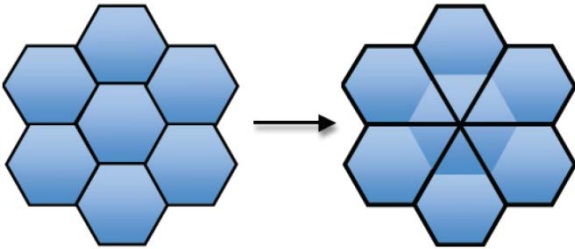
Another feature of the connection free energy is that it allows degeneration. For instance, hexagons can evaporate, leaving a vertex with higher multiplicity. To see this, consider a regular hexagonal tiling, with one of the hexagons, say  $H$ , centred at the origin, all having unit length sides. Let  $0 < \lambda < 1$  and consider  $\lambda H$ . The hexagons around  $H$  can be extended to six sided polygons with all internal angles equal to  $2\pi/3$ . This maintains the local criticality. There are only 12 edges affected by this move. Note that the original vertex sum is 24 from those edges meeting some vertex of  $H$ . Replacing  $H$  by  $\lambda H$  and extending in the way described the new vertex sum is  $12\lambda$ , from the edges of  $\lambda H$ , and a contribution of  $12 \times (2 - \lambda)$  from the edges that lie in the modified hexagons surrounding  $\lambda H$ . The vertex sum has not changed. Though 6 vertices will eventually disappear—to be replaced by one.

In the same manner irregular hexagons with all internal angles  $2\pi/3$  can shrink, to regular isosceles triangles or other polygons all of whose internal angles are  $2\pi/3$  or  $\pi/3$ . One can easily deduce a recipe for the degeneration (production of defects) as illustrated below.



DEFECTS ARISING.

One sees that, for instance Pentagons arise from defect formation. Of course, if something can disappear without energy being gained, then it can also appear from certain configurations.



PENTAGONS APPEAR AND THE INTERFACIAL ENERGY HAS NOT INCREASED.

Of interest is the fact that nonlinear functionals such as  $\Phi(t) = t^p$ ,  $0 < p$  and  $p \neq 1$  in (22) do not allow this degeneracy and the usual hexagonal packing is rigid (no hexagons can be shrunk).

The sums in question are  $12\lambda^p$  and  $12 \times (2 - \lambda)^p$  which are minimised uniquely at  $\lambda = 1$  independent of  $p$  (as long as it is not equal to 1).

There are a few points worth noting. First, if a hexagon disappears in this relaxation process, then the conformal energy (mean angular distortion) of the entire deformation must blow up. Second, if a hexagon should appear, then the Dirichlet energy must blow up. These two facts are consequences of removable singularity theorems for mappings of finite distortion with distortion function in some integrability class,

see Astala et al, 2010 or Marti et al, 2009. For example;

**Theorem 4.** Let  $\Omega$  be a planar domain and  $\mathcal{U}$  a compact connected subregion which is not a point. There is no non-constant mapping of finite distortion  $f: \Omega \setminus \mathcal{U} \rightarrow \mathbb{R}^2$  which shrinks  $\mathcal{U}$  to a point (so  $f$  has a continuous extension to  $\Omega$  and  $f(\mathcal{U}) = \text{point}$ ) with  $\int_{\Omega \setminus \mathcal{U}} \mathbb{A}(z, f) dz < \infty$ .

Of course associated with this observation is the more difficult question of precisely what integrability classes for the distortion are necessary for the conclusion of this theorem, and then the associated extremal problems. These are discussed in (Astala et al, 2010) and the references therein, and so we do not pursue the (quite technical) matter here.

### Simulations of Degeneracy

The data consists of

- A domain  $\Omega$  tiled by regular hexagons  $\Omega = \bigcup_{i=1}^N H_i$
- A boundary deformation  $f_0: \partial\Omega \rightarrow \partial\Omega$ .

#### 1) Algorithm

**Step 1.** Extend  $f_0$  into the domain  $\Omega$  via the Poisson integral of the inverse boundary values so as to minimise mean angular distortion. This gives a configuration of trivalent vertices linked by arcs.

**Step 2.** Minimise the new configuration by evolving the interfacial free energy subject to the constraint that the boundary vertices do not move (Here, energy minimisation was performed using surface evolver (Brakke, 1996).

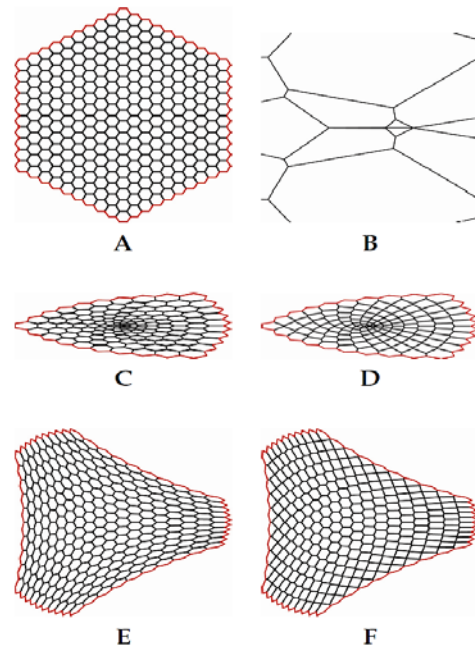


FIG 4 DEFORMATION SOLUTIONS FOR  $\Phi(t) = t^{1/2}$ . A. THE INITIAL HEXAGONAL MESH, THE BOUNDARY IS COLOURED RED. B. ZOOM OF THE CENTRE OF A. C. HARMONIC DEFORMATION  $z \mapsto z^2 + \frac{1}{2} \bar{z}^2$  OF A. D. RELAXED CONFIGURATION OF C. E. HARMONIC DEFORMATION  $z \mapsto z + \frac{1}{2} \bar{z}^2$  OF A. F. RELAXED CONFIGURATION OF E.

The results of this procedure for some harmonic



maps are shown in Fig. 4. At a critical point the internal valency is three and the internal angles are all near  $2\pi/3$  and all the interfaces are line segments. This gives a “deformed hexagonal” packing.

## 2) Extending over the Cellular Structure

At this point we are in the following situation with our model. We have

- A domain  $\Omega$  tessellated by regular hexagons and a boundary map  $f_0$ .
- A polygonal mesh in  $\tilde{\Omega}$  of minimum interfacial energy, and a correspondence between each hexagon  $H$  in  $\Omega$  and a cell (polygon)  $\mathcal{P}_H$  of  $\tilde{\Omega}$ . This correspondence maps the vertices of  $H \in \Omega$  to vertices of  $H \in \tilde{\Omega}$ .

Define a map  $f_H: \partial H \rightarrow \mathcal{P}$  by the linear extension of the vertex values. We now want to fill in the map on  $H$  by the solution of a variational problem to be solved. This problem should reflect a posited internal cellular structure. The filled in map will then be the solution to a second order elliptic equation arising as the Euler-Lagrange equations for the variational problem.

The existence of this map can be obtained for the sorts of equations described at (19) using the theory of  $\mathcal{A}$ -harmonic functions, see Section 6 in Heinonen et al, 1993.

As a first way to advance the model we consider the case where there is no internal structure, and minimise mean angular distortion (or Dirichlet energy of the inverse). In particular we consider the case of harmonic mappings. Chouquet's Theorem (Duren, 2004) implies that the harmonic extension of the piecewise linear boundary values on each hexagon is a smooth (real analytic) diffeomorphism on each cell.

The map is not linear in general and the gradient does not vanish on the interior, in particular. In fact somewhat more is true. First, since each cell is a simply connected region we have the representation of a harmonic function as

$$f_H(z) = \varphi(z) + \overline{\psi(z)}, \quad (24)$$

where  $\varphi$  and  $\psi$  are holomorphic. The Beltrami coefficient, see (7), is

$$\mu(z) = \frac{\varphi'(z)}{\psi'(z)}, \quad (25)$$

but now note that

$$|\mu(z)| = \left| \frac{\varphi'(z)}{\psi'(z)} \right|. \quad (26)$$

Thus the absolute value of the Beltrami coefficient is actually the modulus of an analytic function, and therefore satisfies the maximum principle. Therefore the maximal angular distortion occurs on the boundary (it may not in fact be achieved on the boundary). This shows that the places where the angular distortion occur are confined to the interfacial region.

**Theorem 5.** *The local maxima of the angular distortion of the solution  $f$  are confined to the interfacial structure.*

## Persistence of the Interface

The next natural question that arises is whether or not the interface is encoded in the global deformation that has been found. Basically we ask the following question: if we are given a global minimiser of the process we have described (filling in the cellular structure by harmonic or inverse harmonic mappings), is it possible to recover the initial hexagonal packing (and therefore its image). We might expect the answer is affirmative in general, as for instance the maximal distortion is supported on this set. Of course, the interface could not be reconstructed if the deformation started out with the identity as boundary values. The identity would then be the global minimiser and there is no structure from which we might recover the internal interface.

However the aim of this section is to show that this is about the only case where this occurs. In fact the constructed minimiser has the interface as a sort of second order Sobolev singularity.

**Theorem 6.** *Let  $f$  be the map deforming a hexagonal packing. Then  $f$  fails to lie in the Sobolev space  $W^{2,1}$  across each edge of any polygon, unless  $f$  is the identity.*

To establish this result we first note that if the interior angles are to be preserved, then such a map - if linear - will be the identity. Next, the deformation is harmonic away from the edges and in the Sobolev space  $W_{loc}^{1,1}$  at least. Thus  $\Delta f = 0$  away from the vertices by Weyl's lemma so in particular  $f$  (or its inverse) will be harmonic away from the vertices - so smooth across the edges. But the removable singularity theorem for harmonic maps (in the easiest form) states that if  $f$  is harmonic away from an isolated point and continuous over that point, then it is actually harmonic over the point. In particular the singularities cannot be confined to vertices. In summary, if the map has  $W_{loc}^{1,1}$

regularity across the interface, the mapping is harmonic in a neighbourhood of some hexagon. This, however, is impossible and will be shown momentarily. We want to note here that versions of Weyl's theorem is true for a wide class of second order elliptic equations (assuming  $W^{1,p}$ -regularity for some, often large,  $p$ ) as is the removable singularity theorem (which is typically just an integral estimate using continuity).

The following theorem and its proof hold in much wider generality, but is used to confirm the situation at hand.

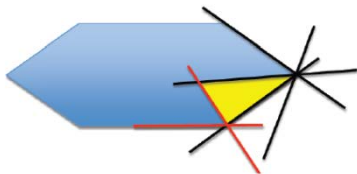
**Theorem 7.** *Let  $\mathcal{P}$  and  $\tilde{\mathcal{P}}$  be hexagons. Let  $h: \mathcal{P} \rightarrow \tilde{\mathcal{P}}$  be a harmonic map with piecewise linear boundary values. Then  $h$  does not extend to a harmonic map of any neighbourhood of  $\mathcal{P}$  unless  $h$  is linear.*

*Proof:* Suppose there is such an extension. Applying a little geometric observation whose proof will lead too far astray (but which is clear in the setting)

**Lemma 1.** *Let  $\mathcal{P}$  be a convex polygon. For  $v$  a vertex and  $E_v$  an edge containing  $v$ ,*

$$E_v = \{v + te^{i\Phi}, t \in [0, s]\},$$

*with internal angle  $\theta$  at  $v$  we let  $\mathcal{R}_v$  denote all the rays  $v + te^{i\Phi+k\theta}$ ,  $k \in \mathbb{Z}$ . Then there are vertices  $v_1, v_2 \in \mathcal{P}$  on an edge, and rays  $\mathcal{R}_1 \in \mathcal{R}_{v_1}$  and  $\mathcal{R}_2 \in \mathcal{R}_{v_2}$  forming a triangle in  $\mathcal{P}$ . The situation is illustrated below.*



A TRIANGLE FORMED BY RAYS.

Returning to the proof, if  $h$  has a harmonic extension over a vertex, then there is a power series expansion. After rotating and scaling (which will certainly not affect the statement of the theorem) one may assume  $[0, 1]$  is an edge of both  $\mathcal{P}$  and  $\tilde{\mathcal{P}}$  and  $h(0) = 0, h(1) = 1$ . So

$$h(z) = az + b\bar{z} + \varphi(z), \quad \varphi(z) = \sum_{k=2}^{\infty} a_k z^k + \bar{b}_k \bar{z}^k \quad (27)$$

A simple first order analysis tells that in fact on the two edges with common vertex 0 we must have  $h(z) = az + b\bar{z}$  (and consequently  $b = 1 - a$ ). Thus  $\varphi$  must vanish along these edges. Substituting  $y = 0$  shows

$$0 \equiv \varphi(z) = \sum_{k=2}^{\infty} a_k z^k + \bar{b}_k \bar{z}^k,$$

which gives, by uniqueness of power series expansions,  $-a_k = \bar{b}_k$  and the formula

$$\varphi(z) = \sum_{k=2}^{\infty} a_k (z^k - \bar{z}^k). \quad (28)$$

Next, for exactly the same reasons as above,  $\varphi$  must vanish on the line  $\{te^{i\Phi}; t \in \mathbb{R}\}$ , where  $\Phi$  is the internal angle at 0 of  $\mathcal{P}$ .

$$0 \equiv \varphi(z) = \sum_{k=2}^{\infty} a_k t^k (e^{ik\Phi} - e^{-ik\Phi}). \quad (29)$$

This gives

$$a_k \sin(k\Phi) = 0. \quad (30)$$

Observe that the following is immediately implied

**Lemma 2.** *If the internal angle  $\Phi$  at any vertex is not a rational multiple of  $\pi$ , then  $h$  is linear.*

And the proof is simply to observe that in those circumstances  $a_k = 0$  for all  $k$ . This was known earlier and can be established via repeated application of the reflection principle and the observation that the level curves of the harmonic map are real analytic curves.

Returning to the proof, observe the further implication of (28) and (30) that

$h$  is the same linear map on all of the rays  $te^{ik\Phi}, t \in \mathbb{R}$ .

This of course holds at every vertex. The lemma finds an edge and a pair of rays (one might be an edge) forming a triangle  $T$  on which  $h$  is piecewise linear (but linear on each edge). It is then an elementary exercise to see that such piecewise linear map always is the restriction of a linear map  $L(z)$  (not true for general polygons, but true for triangles!)—there is a linear map from any triple of non-colinear points to any other such triple. Then  $h(z) - L(z)$  is harmonic on  $\mathcal{P}$  and vanishes on the boundary of the triangle  $T$ . A harmonic function vanishing on the boundary of a simply connected domain is identically 0 in that domain. Then  $h(z) - L(z)$  is real analytic and vanishes in the open set  $T$ . Thus  $h(z) \equiv L(z)$ .

### No Global Periodic Minimiser

In this brief section we consider the large scale problem where we have tessellations of the plane  $\mathbb{R}^2$  and ask about global minimisers preserving hexagonal packings with translational symmetry. In the following theorem the groups  $\Gamma_i$  need not be the full automorphism groups of the packing, just

transitive on the cells.

**Theorem 8.** Let  $T_1$  and  $T_2$  be periodic tessellations of  $\mathbb{C}$  with finite cells and with automorphism groups  $\Gamma_1$  and  $\Gamma_2$  respectively. So the group of translations  $\Gamma_i$  permute the cells of the tessellation.

Let  $\mathbb{C}$  be a fundamental cell in  $T_1$ . There is no solution to the minimisation problem for mean angular distortion

$$\min_{f \in \mathcal{F}} \int_{\mathbb{C}} \mathbb{A}(z, f) dz, \quad (31)$$

where  $\mathcal{F}$  consists of all  $W_{loc}^{1,2}$  homeomorphisms  $f: \mathbb{C} \rightarrow \mathbb{C}$  preserving the tessellations in the sense that for each  $z \mapsto z + \gamma \in \Gamma_1$  there is  $z \mapsto z + \tilde{\gamma} \in \Gamma_2$  such that

$$f(z + \gamma) = f(z) + \tilde{\gamma}, \quad (32)$$

unless there is a linear mapping  $z \mapsto az + b\bar{z} + c$  transforming the tessellations.

Indeed, there are no critical points at all for the variation of (31).

*Proof:* Since  $f$  is a local minimiser, it follows that  $g$  is a local minimiser for the Dirichlet functional  $\int \|Dg\|^2$ . That is (with the regularity assumptions)  $g$  is harmonic. Next, the mapping  $g$  is easily seen to have similar automorphic properties as  $f$  with respect to the groups  $\Gamma_1$  and  $\Gamma_2$ .

$$g(z + \tilde{\gamma}) = g(z) + \gamma, \quad z \mapsto z + \gamma \in \Gamma_1, \quad z \mapsto z + \tilde{\gamma} \in \Gamma_2. \quad (33)$$

Since  $g$  is harmonic,  $g_{z\bar{z}} \equiv 0$ . That is  $g_z$  satisfies the Cauchy-Riemann equations and is therefore analytic. Notice also that therefore

$$g_z(z + \tilde{\gamma}) = g_z(z), \quad (34)$$

and therefore that  $|g_z|$  is periodic and attains its maximum value on any cell such as  $\mathbb{C}$ . Hence  $g_z$  is a bounded entire function which must be constant by the classical Liouville's theorem. The same must also be true of the bounded anti-analytic function  $g_{\bar{z}}$ . Therefore both  $g_z$  and  $g_{\bar{z}}$  are constant on  $\mathbb{C}$  and the map  $g$  is linear.

**Corollary 1.** With the hypotheses of Theorem 8. There is no solution to the minimisation problem

$$\min_{f \in \mathcal{F}} \int_{\mathbb{C}} \|Df(z)\|^2 dz,$$

(a harmonic mapping) unless there is a linear mapping  $z \mapsto az + b\bar{z} + c$ ,  $a, b, c \in \mathbb{C}$  transforming the tessellations.

## Linear Deformations

Here we examine the case of the linear deformation of

a regular hexagonal ray. In models of shearing a cellular structure (as indicated below), it is quite surprising how much symmetry and regularity is retained in the solution.

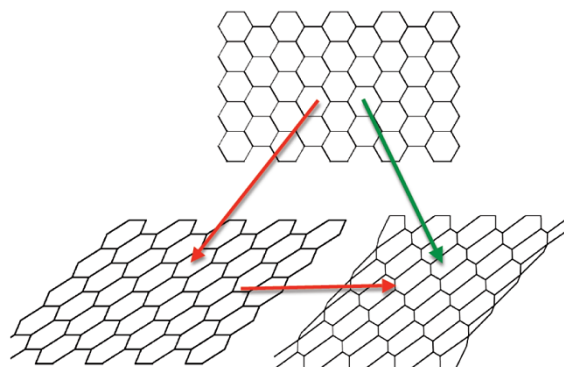


FIG 5 DEFORM BY LINEAR MAP, RELAX INTERFACIAL ENERGY, EXTEND BY HARMONIC MAP. NOTE THAT WE GAIN LOCAL 3-FOLD SYMMETRY

The procedure Algorithm 1, reduces the sum of the internal edge lengths, but the total Dirichlet energy has increased (since the linear mapping is harmonic it clearly minimises total energy for its boundary values).

**Note.** This behaviour is not typical for variational minimisation problems. We have already discussed how Morrey's notion of quasiconvexity is key and would suggest that for shearing the linear boundary values should have a linear minimiser.

One can quite easily see how this symmetry is maintained in the shear mapping. As the boundary values are linear, the harmonic extension of the inverse is also linear.

As an example, consider the shear  $(x, y) \mapsto (x + 1, y)$  on the line  $y = 1$  holding the base  $y = 0$  fixed. The extension minimising mean angular distortion (and in fact maximal distortion) is the linear map  $(x, y) \mapsto (x + y, y)$ . This moves all the vertical lines on which hexagonal edges and vertices lie to have slope 1 while preserving the horizontal lines acting as a translation on each.

A local minimum of the functional  $\mathcal{E}_L$  is found by moving vertices up and down lines of slope 1. The vertices on the upper boundary remaining fixed. The image of an initial cell is then a hexagon all of whose interior angles are  $2\pi/3$  with four opposite edges the same length and two edges stretched.

The harmonic extension of the piecewise linear boundary values effecting this map between cells preserves the slope 1 effect, by symmetry. That is the vertical lines through a pair of vertices are also

mapped to lines of slope 1.

When put together we find the minimiser has the property that the all the vertical lines through vertices are mapped to lines of slope 1.

This is a fairly general picture of what happens for other linear deformations as well. In order to see where the maximal distortion is, and how it is distributed, we need to find this harmonic map between the cells. This is done in the next section.

### The Mapping on a Hexagon

In order to better understand the internal cellular structure after the deformation, the harmonic maps that have been used need to be determined. Fortunately in this regular situation this can be done explicitly.

The conformal mapping from the unit disk  $\mathbb{D} = \{z: |z| < 1\}$  onto a regular hexagon is defined by the Schwartz-Christoffel mapping

$$\varphi(z) = \int_0^z \frac{1}{(1-z^6)^{1/3}}. \quad (35)$$

In this case the image hexagon has side length

$$\ell = \frac{1}{2^{2/3} \cdot 3} \frac{\Gamma^2(\frac{1}{3})}{\Gamma(\frac{2}{3})}, \quad (36)$$

and the 6 sixth roots of unity are mapped to the vertices of the hexagon.

The aim is to describe a particular harmonic map from  $\mathbb{D}$  to the elongated hexagon  $\tilde{\mathcal{P}}$ . Suppose the boundary values are parameterised by a function  $h_0: \mathbb{S} \rightarrow \tilde{\mathcal{P}}$ .

Then the Poisson integral formula gives

$$\Psi(z) = \frac{1}{2\pi} \int_{-\pi}^{\pi} \frac{1-|z|^2}{|e^{it}-z|^2} h_0(e^{it}) dt. \quad (37)$$

From this formula it is evident that if the boundary values satisfy the requisite symmetries, then so does the conformal mapping.

Consider a harmonic map from the regular hexagon  $\mathcal{P}$  to  $\tilde{\mathcal{P}}$ . In order to have the requisite symmetries and continuity of the map obtained by extending via these symmetries, the edges cannot be sheared. One can expect therefore that the following map is near an energy minimiser - it is simply the obvious linear map piecewise defined on the edges.

The hexagon  $\mathcal{P}$  has all side lengths  $\ell$  and maps to  $\tilde{\mathcal{P}}$  the hexagon with upper and lower side lengths  $\alpha\ell$  and other side lengths equal to  $\ell$ . The harmonic map can be constructed as follows.

### 1) Step 1

Compute the harmonic mapping defined on the disk to  $\tilde{\mathcal{P}}$ . This is the Poisson integral of the boundary values defined by the function  $h_0$ ,

$$h_0(e^{i\theta}) = \begin{cases} \varphi(e^{i\theta}) + \frac{\ell}{2}(\alpha-1) & \theta \in [-\pi/3, \pi/3] \\ \varphi(e^{i\theta}) - \frac{\ell}{2}(\alpha-1) & \theta \in [2\pi/3, 4\pi/3] \\ \varphi(e^{i\theta}) + (\alpha-1)\Re(\varphi(e^{i\theta})) & \text{elsewhere} \end{cases} \quad (38)$$

The map  $h_0$  simply translates the four edges whose edge-length is that of the regular hexagon (defined by the image of  $\varphi$ ), and scales the upper and lower edges.

### 2) Step 2

Calculate that (keeping track of orientation)

$$\begin{aligned} & \frac{1}{2\pi} \int_{-\pi}^{\pi} \frac{1-|z|^2}{|e^{it}-z|^2} h_0(e^{it}) dt \\ &= \frac{1}{2\pi} \int_{-\pi/3}^{\pi/3} \frac{1-|z|^2}{|e^{it}-z|^2} \left( \varphi(e^{it}) + \frac{\ell}{2}(\alpha-1) \right) dt \\ &+ \frac{1}{2\pi} \int_{2\pi/3}^{4\pi/3} \frac{1-|z|^2}{|e^{it}-z|^2} \left( \varphi(e^{it}) - \frac{\ell}{2}(\alpha-1) \right) dt \\ &+ \frac{1}{2\pi} \int_{-\pi}^{-2\pi/3} \frac{1-|z|^2}{|e^{it}-z|^2} \left( \varphi(e^{it}) - \frac{\ell}{2}(\alpha-1) \right) dt \\ &+ \frac{1}{2\pi} \int_{\pi/3}^{2\pi/3} \frac{1-|z|^2}{|e^{it}-z|^2} \left( \varphi(e^{it}) + (\alpha-1)\Re(\varphi(e^{it})) \right) dt \\ &+ \frac{1}{2\pi} \int_{-2\pi/3}^{-\pi/3} \frac{1-|z|^2}{|e^{it}-z|^2} \left( \varphi(e^{it}) + (\alpha-1)\Re(\varphi(e^{it})) \right) dt \\ &= \frac{1}{2\pi} \int_{-\pi}^{\pi} \frac{1-|z|^2}{|e^{it}-z|^2} \varphi(e^{it}) dt \\ &+ \frac{\ell}{4\pi} (\alpha-1) \int_{-\pi/3}^{\pi/3} \frac{1-|z|^2}{|e^{it}-z|^2} dt \\ &- \frac{\ell}{4\pi} (\alpha-1) \int_{2\pi/3}^{4\pi/3} \left( \frac{1-|z|^2}{|e^{it}-z|^2} + \frac{1-|z|^2}{|e^{-it}-z|^2} \right) dt \\ &+ \frac{\alpha-1}{2\pi} \left( \int_{\pi/3}^{2\pi/3} \frac{1-|z|^2}{|e^{it}-z|^2} \Re(\varphi(e^{it})) dt \right. \\ &\left. + \int_{-2\pi/3}^{-\pi/3} \frac{1-|z|^2}{|e^{it}-z|^2} \Re(\varphi(e^{it})) dt \right). \end{aligned}$$

Note that the first term in the last equality is the Poisson integral of the boundary values of  $\varphi$  which is conformal and therefore harmonic. By the uniqueness of harmonic mappings with prescribed boundary values, this term must be  $\varphi$  itself

$$\frac{1}{2\pi} \int_{-\pi}^{\pi} \frac{1-|z|^2}{|e^{it}-z|^2} \varphi(e^{it}) dt = \varphi(z). \quad (39)$$

The next term is in fact the harmonic measure of the sectors  $[-\pi/3, \pi/3] \cup [-\pi, -2\pi/3] \cup [2\pi/3, \pi]$  viewed from the point  $z$ . The term is

$$\begin{aligned} \int_{-\pi/3}^{\pi/3} \frac{1-|z|^2}{|e^{it}-z|^2} dt &= -2 \arctan \left( \sqrt{3} \frac{1-|z|^2}{1-4x+|z|^2} \right), \\ - \int_{2\pi/3}^{4\pi/3} \left( \frac{1-|z|^2}{|e^{it}-z|^2} + \frac{1-|z|^2}{|e^{-it}-z|^2} \right) dt &= \\ &+ 2 \arctan \left( \sqrt{3} \frac{1-|z|^2}{1+4x+|z|^2} \right), \end{aligned}$$

and sums to

$$2 \arctan \left( \frac{2\sqrt{3}(1-|z|^2)x}{1-|z|^2+|z|^4-4x^2} \right) \quad (40)$$

Note that one has to be a little careful using these formulae in computation because of the branch



changes where the denominator vanishes.

### 3) Step 3

Solve the remaining final terms involving  $\Re(\varphi)$  to determine the harmonic map.

### The Harmonic Map

Starting with the formula

$$\varphi(z) = \int^z \frac{dz}{(1-z^6)^{1/3}}.$$

Suppose  $z_0 = e^{i\theta}$  with  $\theta \in [\pi/3, 2\pi/3]$ . Because of path invariance of this integral, and if stayed away from the sixthroots of unity (where branch changes will occur), the following is obtained

$$\begin{aligned} \int_0^z \frac{dz}{(1-z^6)^{1/3}} &= \int_0^i \frac{dz}{(1-z^6)^{1/3}} + \int_i^{z_0} \frac{dz}{(1-z^6)^{1/3}} \\ &= i \int_0^1 \frac{dt}{(1+t^6)^{1/3}} + \int_i^{z_0} \frac{dz}{(1-z^6)^{1/3}} \\ &= i \frac{\sqrt{\pi}}{2^{1/3}} \frac{\Gamma(\frac{7}{6})}{\Gamma(\frac{2}{3})} + \int_i^{z_0} \frac{dz}{(1-z^6)^{1/3}}, \end{aligned}$$

and so the real part lies in the second term here. Assuming  $\theta \geq \pi$  (which can be achieved in general by considering the symmetries) and substituting  $z = e^{it}$ ,

$$\begin{aligned} \int_i^{z_0} \frac{dz}{(1-z^6)^{1/3}} &= \int_{\pi/2}^\theta \frac{ie^{it} dt}{(1-e^{6it})^{1/3}} \\ &= i \int_{\pi/2}^\theta \frac{dt}{e^{-it}(1-e^{6it})^{1/3}} \\ &= i \int_{\pi/2}^\theta \frac{dt}{(e^{-3it}-e^{3it})^{1/3}} \\ &= \frac{1}{2^{1/3}} \int_{\pi/2}^\theta \frac{dt}{\sin^{1/3}(3t)} \\ &= -\frac{\cos(3\theta)}{2^{1/3} \cdot 3} {}_2F_1\left(\frac{1}{2}, \frac{2}{3}, \frac{3}{2}, \cos^2(3\theta)\right), \end{aligned}$$

where  ${}_2F_1$  is the hypergeometric function. This gives the following formula.

**Corollary 2.** For  $\theta \in [\pi/3, 2\pi/3]$  one has

$$\begin{aligned} \Re(\varphi(e^{i\theta})) &= \frac{1}{2^{1/3}} \int_{\pi/2}^\theta \frac{dt}{\sin^{1/3}(3t)} \\ &= -\frac{\cos(3\theta)}{2^{1/3} \cdot 3} {}_2F_1\left(\frac{1}{2}, \frac{2}{3}, \frac{3}{2}, \cos^2(3\theta)\right). \end{aligned}$$

Since  $x = \Re(z) = \cos(t)$  and since  $\cos(3t) = 4x^3 - 3x$

$$\varphi(z) = -\frac{x(4x^2-3)}{2^{1/3} \cdot 3} {}_2F_1\left(\frac{1}{2}, \frac{2}{3}, \frac{3}{2}, x^2(4x^2-3)^2\right) \pm i \frac{\ell}{\sqrt{2}}, \quad (41)$$

for  $x = x + iy$ ,  $|z| = 1$ ,  $x \in [-\frac{1}{2}, \frac{1}{2}]$  and where the sign is chosen to be the same as that of  $y$ . Actually, from this and the rotational symmetry of the image hexagon,

one can deduce the boundary values of the conformal map  $\varphi$  at all points.

The required map is  $\Psi(\varphi^{-1}(z)): H \rightarrow \tilde{H}$ . This is

$$\Psi(\varphi^{-1}(z)) = z + g(\varphi^{-1}(z)) = z + h(z), \quad (42)$$

with  $h$  real valued. This shows that the putative minimal energy map should preserve the level lines in the  $y$ -axis.

Note that  $\Re(\varphi(e^{i\theta}))$  is the real part of an analytic function  $\varphi$ , and is therefore harmonic.

### Discussion

Stable configurations of discrete-structures have been found under prescribed boundary conditions. Assuming that energy stored at every  $z \in \text{int}(\Omega)$ , the interior to a cell ( $\Omega$ ) in the discrete structure, is of the form

$A(z)Df$ , and a mapping  $h_0 \in W^{1,2}(\partial\Omega, \mathbb{R}^2)$ , a piecewise linear map on the boundary values of the cell and not the entire domain, we seek the configuration for which the total stored energy (including interfacial terms) is minimal. First we find the interfacial configuration, then minimise

$$\int_{\Omega} A(z) |Df|^2 dz < \infty$$

over all the class of maps  $f \in h_0 \in W_0^{1,2}(\partial\Omega, \mathbb{R}^2)$  on the cell boundary values. For regular  $A(z)$ , the existence of the minimiser is guaranteed by the principles of convex analysis, and the uniqueness depends on the convexity of the operator norm.

It was proved in Theorem 2 that the problems of minimisation of local mean angular distortion and Dirichlet energy are identical (up to a measure). Examples using model energy functionals on hexagonal lattices were proposed and their stable configurations for linear deformations were determined and verified numerically. Note that the results, however, are valid for general lattices.

The results are limited to physical systems that are adequately described using mean angular-distortion or its weighted-mean-distortion extensions. Note that these class of functionals capture a wide range of (non-linear) elastic materials. A potential extension would be to analyse  $p$ -harmonic functionals, with Euler-equation of the type

$$\text{div}(|Df|^{p-2} Df) = 0,$$

which have been shown to describe nonstandard growth conditions (Ruzicka, 2000).

There are significant technical difficulties in using the direct method of variational calculus to analysing these problems for other  $L^p$  –norms.

For instance,  $\int_{\Omega} A^p(z, f) dz$  for  $p \neq 1$  already seems completely intractable. This is a subject for future research.

#### REFERENCES

- Astala, K., Iwaniec, T., and Martin, G. Elliptic partial differential equations and quasiconformal mappings in the plane. Princeton University Press, 2009.
- Astala, K., Iwaniec, T., and Martin, G. "Deformations of Annuli with Smallest Mean Distortion." *Arch. Rational Mech. Anal.* 195: (2010) 899–921.
- Bezdek, A., and Kuperberg, W. "Maximum density spacepacking with congruent circular cylinders of infinite length." *Mathematika* 37, 1: (1990) 74–80.
- Brakke, K. A. "The Surface Evolver and the Stability of Liquid Surfaces." *Phil. Trans. A* 354, 1715: (1996) 2143–2157.
- Cafferelli, L. A., and Lin, F. H. "An optimal partition problem for eigenvalues." *J. Scient. Comput.* 31, 1-2: (2007) 5–18.
- Cybulski, O., and Holyst, R. "Tiling a plane in a dynamical process and its applications to arrays of quantum dots, drums, and heat transfer." *Phys. Rev. Lett.* 95, 8: (2005) 1–4.
- Drenckhan, W., Weaire, D. and Cox, S. J. "The demonstration of conformal maps with two-dimensional foams." *Eur. J. Phys.* 25, 3: (2004) 429–438.
- Duren, P. L. Harmonic mappings in a plane. Cambridge University Press, 2004.
- Engelmayr Jr., G. C., Cheng, M., Bettinger, C. J., Borenstein, J. T., Langer, R. and Freed, L. E. "Accordion like honeycombs for tissue engineering of cardiac anisotropy." *Nature Mat.* 7, 12: (2008) 1003–1010.
- de Gennes, P. G., and Prost, J. *The Physics of Liquid Crystals*. Oxford, Clarendon, 1993, 2 edition.
- Heinonen, J., Kilpeläinen, T. and Martio, O. Nonlinear potential theory of degenerate elliptic equations. Oxford Mathematical Monographs. New York: The Clarendon Press Oxford University Press, 1993. Oxford Science Publications.
- Hencl, S., and Koskela, P. "Regularity of the Inverse of a Planar Sobolev Homeomorphism." *Arch. Rational Mech. Anal.* 180: (2006) 75–95.
- Iwaniec, T., and Martin, G. J. "The Beltrami Equation." *Mem. Amer. Math. Soc.* 191, 893.
- Mancini, M., and Oguey, C. "Foams in contact with solid boundaries: Equilibrium conditions and conformal invariance." *Eur. Phys. J. E* 17, 2: (2005) 119–128.
- Martin, G. J., Astala, K. and Iwaniec, T. "Bilipschitz homeomorphisms of the circle and nonlinear Beltrami equations." *Quaderni di Matematica* 105–117.
- Martio, O., Ryazanov, V., Srebro, U. and Yakubov, E. *Moduli in Modern Mapping Theory*. Springer Monographs in Mathematics. Springer, 2009.
- Morrey Jr., C. B. Multiple integrals in the calculus of variations. Classics in Mathematics. Springer-Verlag, Berlin, 1966.
- Mullins, W. W. "Solid surface morphologies governed by capillarity." *Metal Surfaces* 17–66.
- Oseen, C. W. "The theory of liquid crystals." *Trans. Faraday Soc.* 29: (1933) 883–899.
- Pavlovic, M. "Boundary correspondence under harmonic quasiconformal homeomorphisms of the unit disk." *Ann. Acad. Sci. Fenn. Math.* 27: (2002) 365–372.
- Ruzicka, M. Electrorheological fluids: modeling and mathematical theory, volume 1748 of Lecture Notes in Mathematics. Berlin: Springer-Verlag, 2000.
- Schoen, R. and Yau, S-T. Lectures on harmonic maps. Conference Proceedings and Lecture Notes in Geometry and Topology, II. International Press, Cambridge, MA, 1997.
- Virga, E. G. Variational theories for liquid crystals, volume 8 of Applied Mathematics and Mathematical Computation. Chapman & Hall, London, 1994.
- Von Neumann, J. "Discussion remark concerning paper of C.S. Smith, grain shapes and other metallurgical applications of topology." *Metal Interfaces* 108–110.
- Weaire, D., and Hutzler, S. *The physics of foams*. Clarendon Press, Oxford, 1999.
- Weaire, D., and Rivier, N. "Soap, cells and statistics - Random patterns in two dimensions." *Contemp. Phys.* 50, 1: (2009) 199–239.